AD-A266 260

ATION PAGE

Form Approved
OMB No. 0704-0188

1. AGENCY USE ONLY (Leave blank)	2. REPORT DATE	3. REPORT TYPE AND DATES COVERED
	3 Jun 93	Final Report 01 Jun 92 - 31 Dec 92

4. TITLE AND SUBTITLE
ATOMIC LAYER EPITAXY OF BORON NITRIDE

5. FUNDING NUMBERS
F49620-92-C-0037

6. AUTHOR(S)
Dr M Asif Khan

7. PERFORMING ORGANIZATION NAME(S) AND ADDRESS(ES)
APA Optics Inc
2950 NE 84th Lane
Blaine MN 55449

8. PERFORMING ORGANIZATION REPORT NUMBER
AFOSR-R- [illegible] 8

9. SPONSORING/MONITORING AGENCY NAME(S) AND ADDRESS(ES)
AFOSR/NE
110 Duncan Avenue Suite B115
Bolling AFB DC 20332-0001

10. SPONSORING/MONITORING AGENCY REPORT NUMBER
3005/SS

11. SUPPLEMENTARY NOTES

12a. DISTRIBUTION/AVAILABILITY STATEMENT
UNLIMITED

12b. DISTRIBUTION CODE

13. ABSTRACT (Maximum 200 words)

This document summarizes the work performed under the Phase I project aimed at developing the wide bandgap nitrides for high temperature electronics and optoelectronics applications. The focus was on the study of atomic layer epitaxy of BN, AlN and GaN. We present a summary of the program accomplishments. This is followed by a description of the technical effort including the data obtained. Finally we outline a potential Phase II program.

14. SUBJECT TERMS

15. NUMBER OF PAGES

16. PRICE CODE

17. SECURITY CLASSIFICATION OF REPORT	18. SECURITY CLASSIFICATION OF THIS PAGE	19. SECURITY CLASSIFICATION OF ABSTRACT	20. LIMITATION OF ABSTRACT
UNCLASSIFIED	UNCLASSIFIED	UNCLASSIFIED	UNLIMITED

Atomic Layer Epitaxy of Boron Nitride.

PHASE - I

FINAL TECHNICAL REPORT

Contract No: F49620-92-C-0037

June 3, 1993

Submitted by

Dr. M. Asif Khan

APA Optics, Inc.

2950 N. E. 84th Lane

Blaine, MN 55449

PHASE I FINAL REPORT

Contract Number F49620-92-C-0037

This document summarizes the work performed under the Phase I project aimed at developing the wide bandgap nitrides for high temperature electronics and optoelectronics applications. The focus was on the study of atomic layer epitaxy of BN, AlN and GaN. We present a summary of the program accomplishments. This is followed by a description of the technical effort including the data obtained. Finally we outline a potential Phase II program.

1.0 Key Program Accomplishments

This section briefly describes each of the major accomplishments achieved in the Phase I and the significance toward future work.

1.1 LPMOCVD System For BN Depositions

Our basic contention for single crystal BN deposition was to try high temperature (1100^{o} C) atomic layer epitaxy. We built a unique LPMOCVD system in the program to accommodate this. A unique system design, use of ceramics and water cooled quartz jackets were the key innovations that were implemented. We also incorporated optical windows in the system to evaluate photo-assisted growths and insitu monitor the growing films. The development of BN growth capabilities using the SALE and conventional growth techniques places us in excellent position to conduct future BN-$Ga_xAl_{1-x}N$ growth studies and device development.

Description of these will be provided in the technical details section.

1.2 Atomic Layer Epitaxy of BN

We succeeded in depositing high quality smooth BN films using high temperature atomic layer epitaxy. The kinetics of the BN ALE process were also studied and resulted in some qualitative deductions as to the role of nitrogen desorption during growth. Single crystal hexagonal BN films using atomic layer epitaxy were obtained, however attempts to obtain cubic boron nitride were not successful.

1.3 BN ALE Growth Kinetics Study

We studied the growth rate in BN ALE as a function of growth parameters. This data is significant from the perspective of future device design which requires multilayer depositions under various growth conditions.

1.4 BN-$Al_xGa_{1-x}N$ Heterojunctions Depositions and Characterization

High quality BN-$Al_xGa_{1-x}N$ heterojunctions were deposited in the program. The BN layer served as the insulator in these junctions. These junctions were characterized for their depletion properties using capacitance voltage and current-voltage measurements. We found BN-$Al_xGa_{1-x}N$ heterojunctions to be excellent for the fabrication of MIS devices. Such devices can form the basis of complementary transistor technology based on the wide bandgap nitrides. They therefore can serve as the building blocks for high temperature high performance electronics. This is a significant accomplishment and serves as the basis of future electronic devices.

1.5 PHASE II Device Approach

A metal insulator semiconductor field effect transistor (MISFET) device design was developed for fabrication in the Phase II program. The device was modelled using a computer simulation. Results show the feasibility of fabricating CMOS type devices from the BN-$B_xGa_{1-x}N$ heterojunctions.

1.6 Transistor Fabrication Process Development

For the Phase II device design we successfully developed some key processing steps such as reactive ion etching, ion implantation and contact metallizations. These establish the technical feasibility of our Phase II device approach.

2.0 Technical Details

This section details the technical accomplishments of the Phase I program.

2.1 System Modifications

At the onset of the program, our LPMOCVD system was modified to accommodate a triethylboron (TEB) source. An additional metal organic loop was added to the system configuration along with a bubbler cooling bath capable of keeping the temperature inside the bubbler to within +/- 0.1° C. The growth loop for the boron was connected to the APA fast switching manifold which allows for switched atomic layer epitaxy.

Along with the addition of a boron precursor to the system, a quartz window was added to the top plate of the reactor so laser radiation could be admitted to the epilayer surface during growth. The use of laser assisted growth has recently shown promise of lowering growth temperatures and improving material quality. The quartz window also allows us to monitor the growth surface by measuring the intensity of a reflected visible laser, in this case a HeNe laser. This experimental configuration is displayed in Figure 1. By monitoring the amount of reflected laser light from the surface as a function of

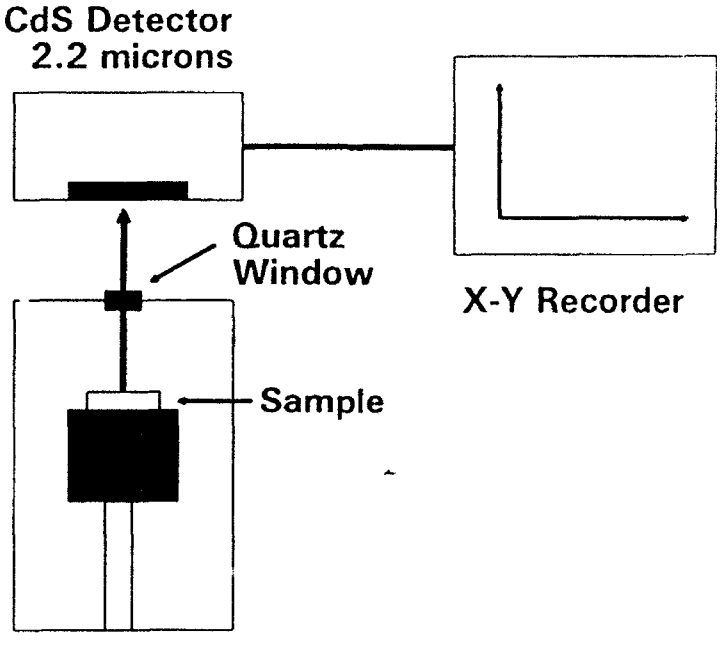

Figure 1. Experimental visible reflectometry setup.

growth time, one can determine the growth rate in situ. Due to interference effects, as the film thickness increases the intensity of the reflected laser beam oscillates. Figure 2 is a measure of reflected laser intensity as a function of time for an 18 period superlattice of GaN and $Al_{0.2}Ga_{0.8}N$. The spectra

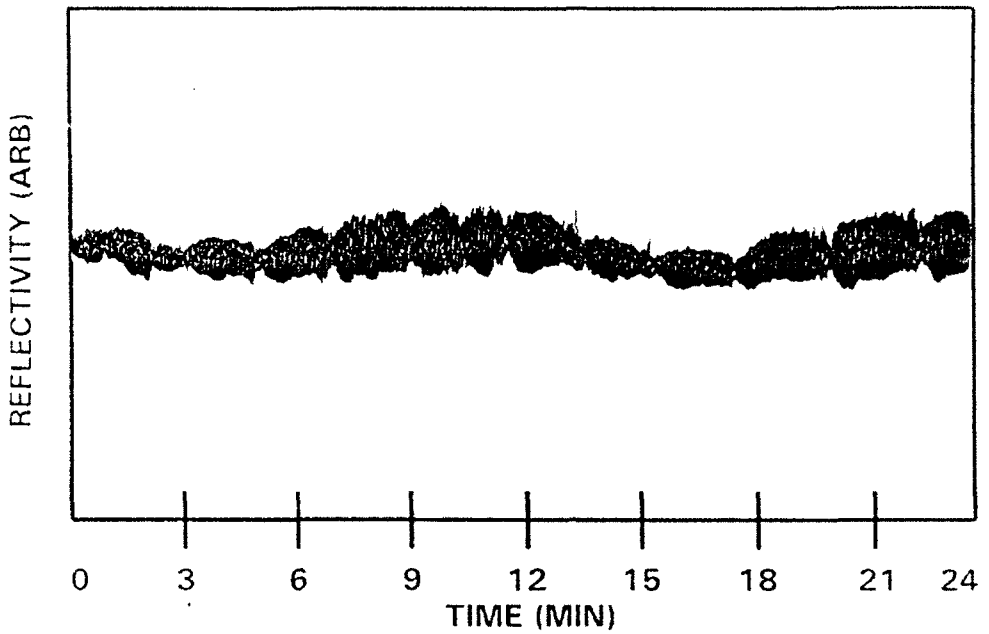

Figure 2. Reflected laser intensity as a function of growth time.

consists of two separate periodicities. The small sausage link like structures arise from the change in surface from GaN and AlGaN which have different reflectance coefficients. The larger periodicity superimposed on the smaller links gives the thickness of the overall structure.

2.2. BN-$Al_xGa_{1-x}N$ Heteroepitaxy and Film Characterizations

All growths performed in Phase I were grown on an APA Optics proprietary low pressure metal organic deposition (LPMOCVD) reactor. This state of the art reactor is fully computer controlled. The reactor allows for the deposition of BN and $Al_xGa_{1-x}N$ using switched atomic layer epitaxy (SALE) or growth under conventional growth where precursors flow continuously. Figure 3 shows how a monolayer of BN is deposited with SALE. The column III precursor, TEB (boron) in this case, is switched into the reactor

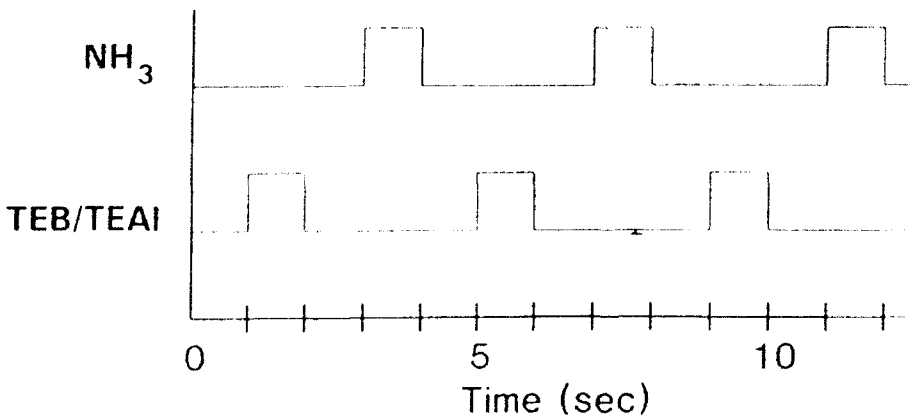

Figure 3. SALE growth sequence for a monolayer of BN.

for an interval of one second. Following this interval, a one second dead zone where no precursors are admitted to the reactor, is done. Ammonia is then pulsed in for one second followed by another dead zone. This cycle is repeated 'X' amount of times to achieve the desired BN thickness.

Some of the initial BN films grown using the SALE approach where found to be nitrogen deficient. This was determined using Auger (AES). A study was conducted where the nitrogen pulse time was increased in 1 second increments to a maximum of three seconds. The anticipated result here was to increase the amount of incorporated nitrogen in the film by lengthening the exposure of the film surface to additional nitrogen. The result of the study indicated the reverse to be true. As the length of ammonia exposure was increased, the less nitrogen was incorporated. These results are based on Auger and transmission studies. Figure 4 shows the transmission spectra for three different BN layers grown with increasing ammonia exposure. Evident is a shift in the cutoff wavelength to higher values as

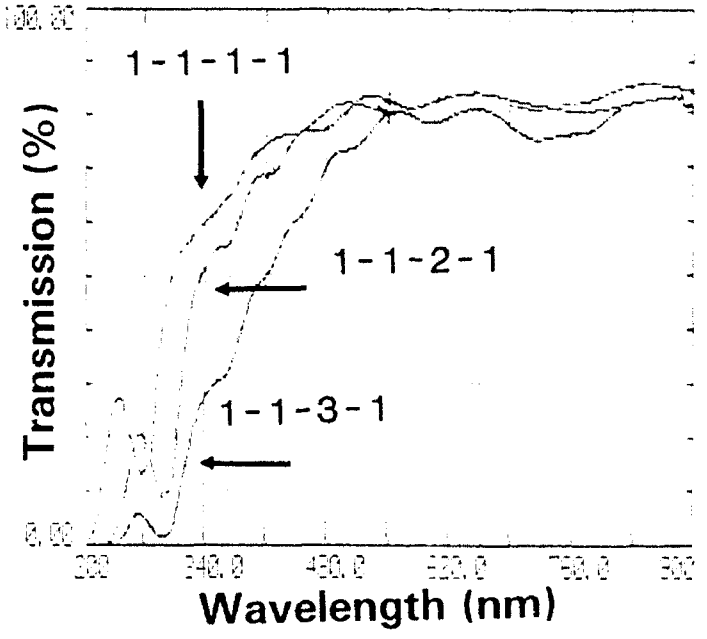

Figure 4. Optical transmission of BN as a function of increasing ammonia exposure during SALE.

the ammonia time was increased. This condition has been reported in literature as the results of nitrogen deficiency in the epilayers.

Based on these results a series of growths were performed which kept the ammonia exposure time constant and increased the dead zone following the TEB exposure. The thought was to allow extra surface boron to desorb leaving the desired one monolayer coverage. Based on growth rate data and transmission studies, the films were found to decrease in thickness and increase in nitrogen content.

In earlier studies of BN epilayers grown conventionally on sapphire substrates, it was found that the epilayers would peal off the sapphire substrate post growth. The time interval for pealing varied from 1 hour to several days depending on how much boron was incorporated in the epilayer. To increase the adherence of the conventionally and SALE grown BN layers to GaN and sapphire surfaces, growth of a 40 X period of BN was performed at low temperatures. Films grown on these buffer layers had excellent adherence.

To determine which phase of BN was grown, an IR spectrometer was used to measure the transmission of BN/Si and BN/Sapphire structures. Depending on the signature of the spectra, the crystal structure of

the BN could be determined as either being hexagonal or cubic. Figure 5 shown below is such a spectra taken on a BN/Si (100) structure grown at 1300° C. Two peaks at 800 and 1400 cm^{-1} indicate the film to be predominantly hexagonal.

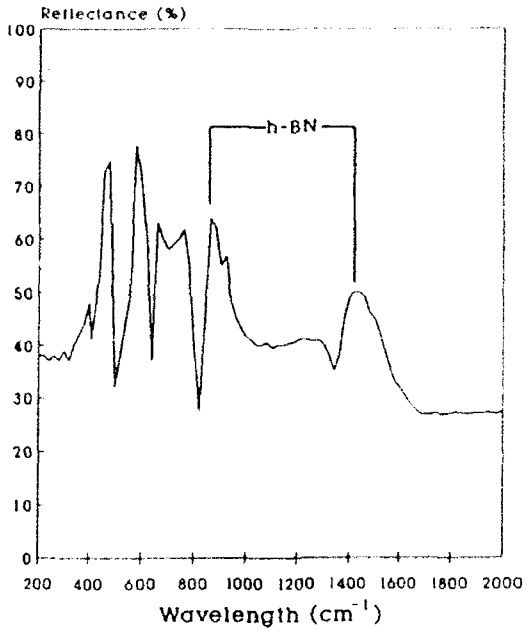

Figure 5. IR transmission spectra of hexagonal BN.

This epilayer was also characterized using x-ray diffraction to determine if the film were single crystal. The x-ray spectra is shown in Figure 6. Evident is a hexagonal peak associated with BN at 23.2 degrees. The c axis lattice constant is slightly larger then the expected lattice constant for BN. The

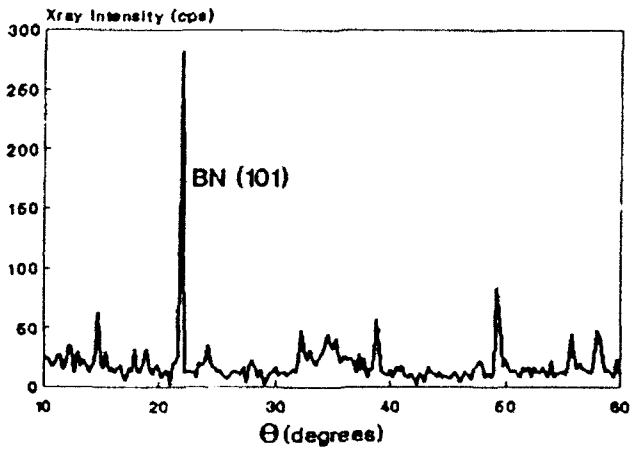

Figure 6. Hexagonal BN x-ray spectra.

cause of this change in lattice constant could be due to the effects of strain in the lattice and the effects of Poissons ratio. Films grown at 1000° C showed no evidence of a hexagonal peak. This data indicates that for single crystal epitaxy of BN higher growth temperatures need to be tried.

Another powerful technique for characterizing the BN epilayers was to perform optical transmission in the visible and UV portions of the spectrum. Hexagonal BN has a bandgap energy of 6.2 eV which corresponds to complete optical absorption for wavelengths less then 200 nm. For wavelengths above the bandgap, (i.e. wavelengths above 200 nm) light is transparent to the material. A study was conducted to measure the optical transmission as a function of wavelength for a series of BN growths on sapphire. The variable in this experiment was the amount of TEB, the boron precursor. Figure 7 shows the measured transmission of these three films. As the amount of boron is increased in the film,

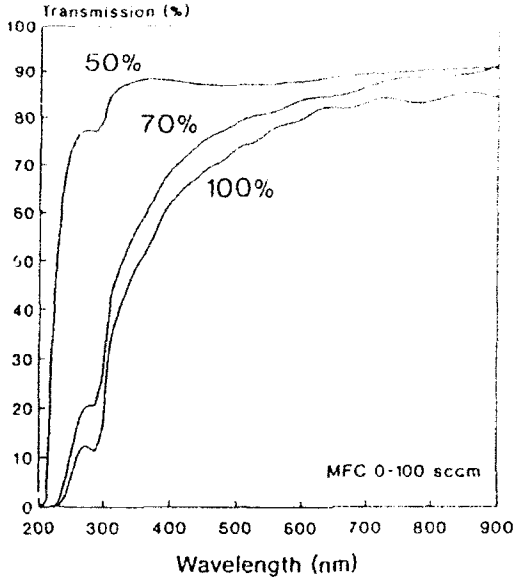

Figure 7. Optical transmission of BN as a function of TEB flow.

the transmission cutoff is seen to increase in wavelength and the cutoff becomes gradual versus a sharp cutoff, as is seen for the top curve. The source of this cutoff shift is the addition of boron above stoichiometry. For a stoichiometric BN layer, the ratio of B to N atoms is 1:1. Another means by which the amount of elemental B and N can be measured is the use of auger electron spectroscopy (AES).

Not only can AES be used to measure the relative amounts of elements in a solid, if can also be used to determine the amounts of contaminants, oxygen and carbon for instance. A stoichiometric layer of BN was grown on a Si(110) substrate and following system removal was transferred to a UHV chamber for AES analysis. Prior to AES measurements, the sample surface was lightly sputtered with Argon atoms to remove any surface contaminants related to transfer. Figure 8 shows the AES spectra for this sample. The spectra clearly shows two large peaks associated with B and N. There is no trace of oxygen in the sample as the primary peak for O is at 503 eV. Similarly, no carbon peak is seen at the expected energy of 272 eV. The results of our AES studies indicate that the films grown under SALE and conventional techniques are extremely clean of contaminants. Auger confirms the transmission studies in that the ratio of B to N in the epilayer increases as the transmission cutoff wavelength increases.

In summary, BN depositions were carried out on Si and sapphire substrates as a function of both growth temperature and growth technique. Hexagonal BN material was obtained using SALE and conventional growths at temperatures of 1300° C. It was determined that a nitrogen deficiency in the BN layers occurred in SALE when the length of the ammonia pulse was increased. Hexagonal layers of BN

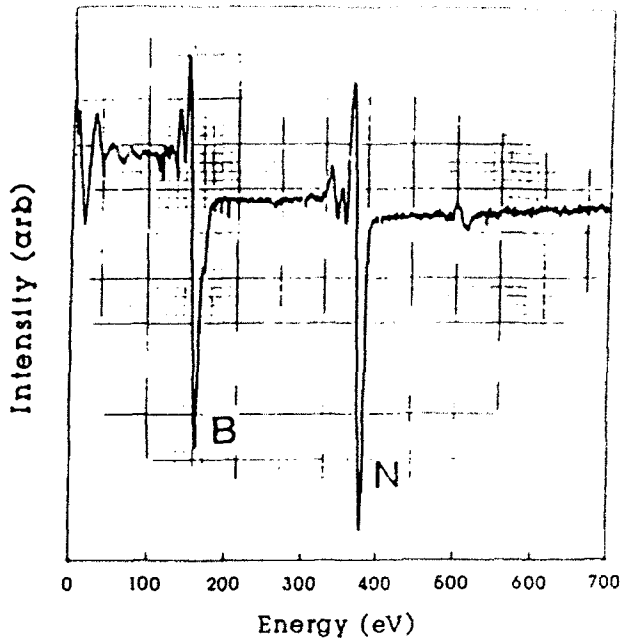

Figure 8. Auger electron spectroscopy spectra of BN layer.

were achieved when the width of the ammonia pulse was kept at 1 second. By increasing the amount of TEB within the pulse time lead to the accumulation of additional boron in the BN film as determined by optical transmission and AES studies. AES also shows that the BN films grown under stoichiometric conditions exhibit a low level of contaminants, within the noise of the instrument, less then one percent in this case.

2.3 BN ALE Growth Kinetics Study

During Phase I, several growth kinetic studies were performed. Along with the SALE results described above, the growth rate of BN was also investigated. Variables studied which could affect the overall growth rate included temperature, lengths of pulses in the SALE growth, amount of hydrogen carrier gas and finally using nitrogen instead of hydrogen as the carrier gas.

BN was grown using an ALE growth sequence of 1313. The B and N precursors were pulsed in for three seconds with a one second dead zone between pulses. Identical layers were grown at 1000 and 1300o C. The measured growth rates were 17.5 and 15.5 angstroms/cycle at 1000 and 1300° C respectively. The overall SALE growth rate was found to vary only slightly with temperature in this temperature region. As mentioned earlier although the growth rate seemed fairly independent of temperature, the material crystallinity improved dramatically with increasing temperature and future work will focus on further increases in the growth temperature.

Another variable which affects the growth dynamics on the surface is the carrier flow rate. The carrier gas in this set of experiments was hydrogen. The flow rate of the carrier gas can radically affect the conditions on the surface of the substrate since for increasing flow rates the velocity of arriving atoms increases, thus limiting the time for reaction before the reactants are carried away. In this experiment, BN was grown using the SALE process using a 1131 cycle. Here a 3 second dead zone was installed following the TEB pulse and a one second dead zone following the ammonia pulse. The growth temperature for this series of experiments was 1000° C. Two identical runs were conducted where the hydrogen carrier flow rate was 1.5 and 0.75 slm. The growth rates were 17.5 and 60 angstroms/cycle for hydrogen flow rates of 1.5 and 0.75 slm respectively. The rapid increase in growth rate observed with

the lowering of carrier gas flow confirms the notion that the carrier velocity is very important and that by reducing this velocity the growth rate is increased.

In a separate study, nitrogen was used to replace hydrogen as the carrier gas. Since nitrogen desorption is a problem in the growth of BN, due to the high equilibrium vapor pressure of nitrogen over BN surfaces, the experiment studied what effect the presence of free nitrogen (N_2) would have on the growth rate of BN. BN was grown using SALE at 1000 and 1300° C using conditions which deposited BN earlier using hydrogen as the carrier. In both cases no deposition occurred. For this reason the use of nitrogen as a carrier gas was abandoned.

These series of experiments demonstrate several of the controlling variables and the effects they have on BN growth. Based on these data, successful growth of BN should be grown using hydrogen as the carrier gas and should occur at the highest growth temperature possible for either conventional or SALE growth.

2.4 BN-$Al_xGa_{1-x}N$ Heterojunction Deposition and Characterization

All MISFET structures in Phase I were grown using the LPMOCVD reactor described earlier. Growth techniques included both conventional and SALE. The typical MISFET structure grown during Phase I is shown in Figure 9. This structure consists of a GaN conduction channel capped with either BN,

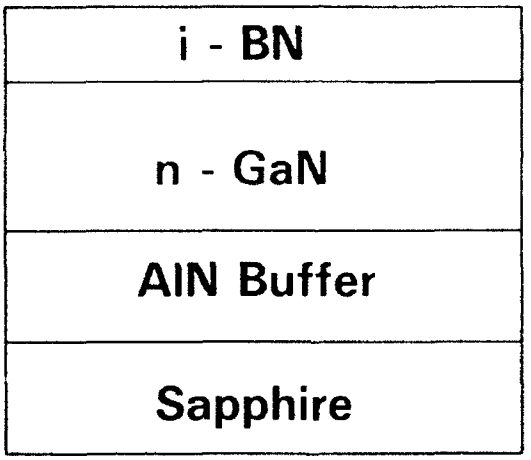

Figure 9. Typical MISFET structure.

$Al_xGa_{1-x}N$, or a combination of the two. These structures were typically grown at 1000_o C. The structures grown in Phase I were characterized using Auger electron spectroscopy (AES), reflection high energy electron diffraction (RHEED), capacitance - voltage (C-V) and current - voltage (I-V) measurements.

2.4.1 $Al_xGa_{1-x}N$/GaN MISFET Characterization

Prior to device fabrication, MISFET structures were evaluated using a mercury C-V probe. This measurement allows the non-destructive measurement of the doping concentration as a function of

depletion depth. Figure 10 shows a typical C-V plot for a MISFET. Carrier concentration and depletion depth are plotted as a function of depletion voltage. In this particular case 4000 angstroms of n-type

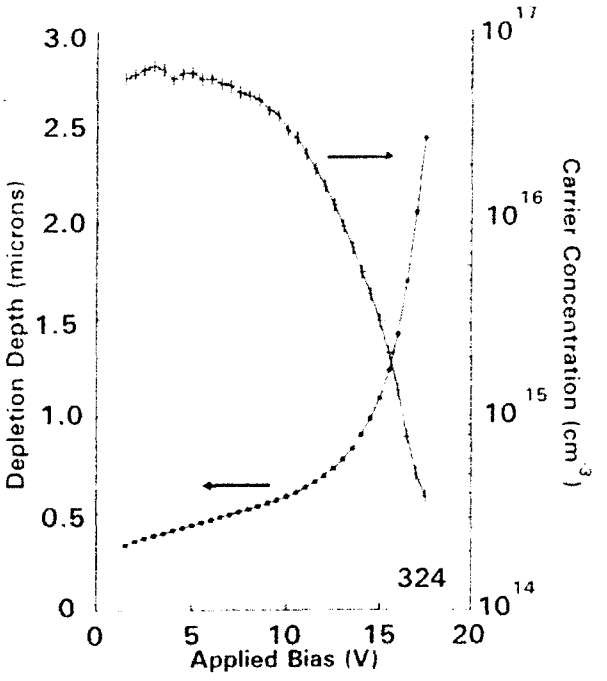

Figure 10. Carrier concentration and depletion depth vs. applied bias for a MISFET structure.

GaN was grown on an insulating buffer layer. The surface of the channel was capped with a 200 angstrom layer of AlN. At a depletion bias of -10 volts, the depletion depth is seen to increase dramatically as the carrier concentration decrease rapidly. The bias at which this occurs marks the point at which the conduction channel has been completely depleted of electrons. This point is often referred to as pinchoff.

Due to the considerable strain in the AlN insulator layer, the thickness of the AlN is limited to a value below the critical layer thickness. For thick films of AlN, 500 angstroms, insulator relaxation was seen to occur and the results of C-V measurements indicated that the depletion depth was pinned at the interface of the AlN and GaN. The cause of this pinning is due to the large number of defects generated following film relaxation. The pinning of the depletion depth is fatal to device operation since the width of the conduction channel cannot be modulated.

Interestingly, it was discovered that if a relaxed layer of AlN was grown on GaN followed by the deposition of a thin BN on the AlN layer, the depletion depth became unpinned. The unpinning of the depletion depth allowed for the depletion of the conduction channel. Figure 11 shows the depletion depth as a function of applied bias for a MISFET structure with a thin BN cap. As seen depletion depth continues to increase with increasing applied bias. If the depletion depth were pinned in this example, the depletion depth would have been fairly constant as a function of bias. This result is extremely encouraging for future MISFET developments.

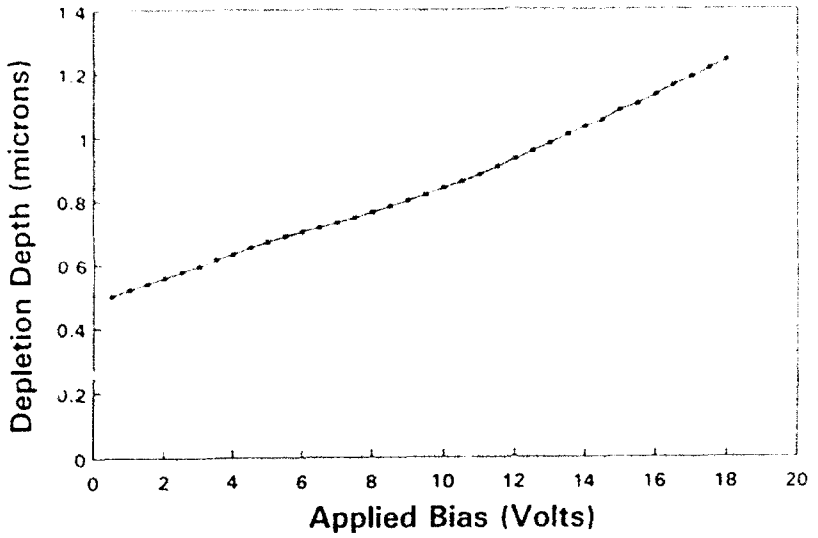

Figure 11. Carrier concentration and depletion depth vs applied bias for a MISFET structure with a BN cap.

2.5 Phase II Device Approach

This section describes the proposed Heterojunction Insulator Gate Field Effect Transistor (HIGFET) device to be fabricated and evaluated during Phase II. Preliminary modelling efforts are also described in detail.

The proposed HIGFET device is schematically shown in Figure 12. The structure consists of an AlN buffer layer on which a 200 angstrom n-type GaN channel is grown. The doping in the channel is 1 X

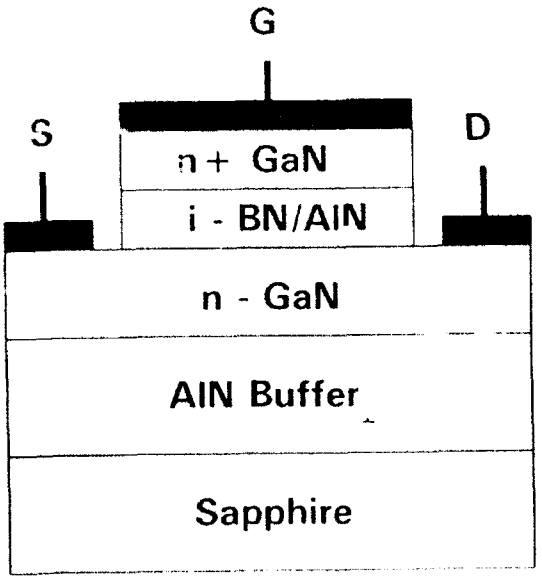

Figure 12. Proposed HIGFET device for Phase II.

10^{17} cm^{-3}. Following the channel growth, a 200 angstrom insulating layer of BN is grown to isolate the gate metallization from the channel. Note the gate insulator could also be a combination of AlN and BN both excellent insulators. A thin layer of highly doped n-type GaN is grown on the AlN to facilitate gate metallization. The dimensions of the device are: gate length 4 microns, GaN quantum well 200 angstroms, AlN gate insulator 200 angstroms. The location of the source and drain ohmic metallizations are located as close to the gate region as possible without contact. The source and drain ohmic contacts are defined in a reactive ion etching step and are patterned using a standard photolithography process.

With these device parameters, the device I-V characteristic curves were modelled using the following values: V_t = -0.16 V (threshold) e_{AlN} = 8.1 X 10^{-11} F/m, u = 420 $cm^2V^{-1}s^{-1}$, and v_{sat} = 10^5 m/s and are shown in Figure 13. The expected transconductance for this HIGFET is 125 mS/mm.

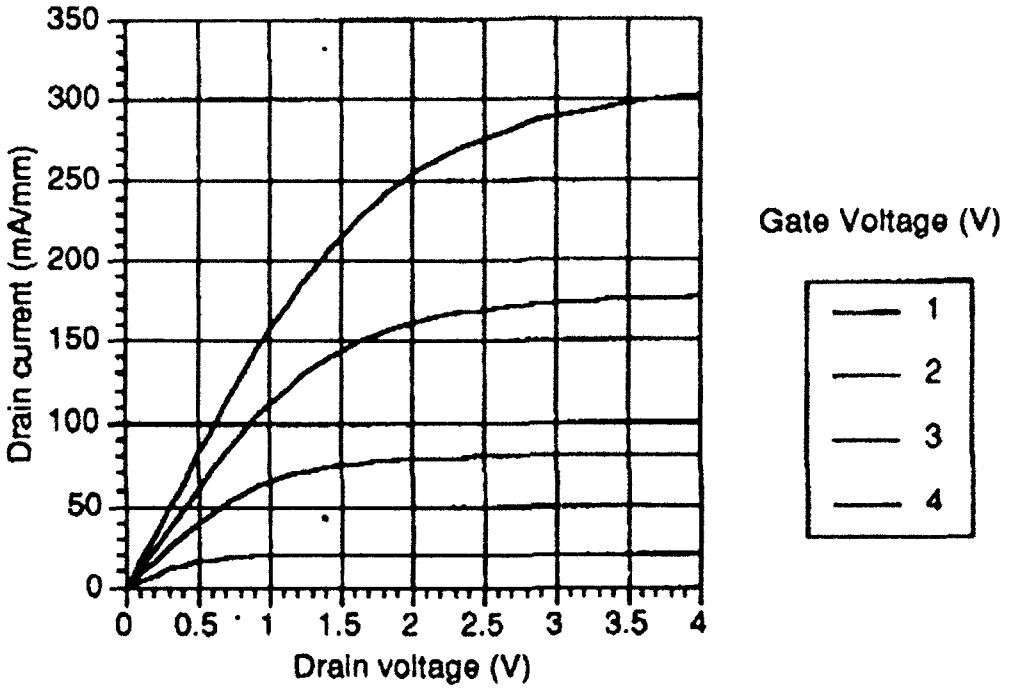

Figure 13. Modelled I-V characteristics for HIGFET device.

2.6 BN-$Al_xGa_{1-x}N$ MISFET Process Development

The following section describes the process steps required in the fabrication of a BN-$Al_xGa_{1-x}N$ based MISFET device. These steps include MESA definition and isolation, ohmic and Schottky metallizations and device evaluation.

2.6.1 Reactive Ion Etching of Nitrides.

The first step in the fabrication of a MISFET is the MESA isolation step. This step is needed to define the device area and to isolate the devices from each other. To fabricate the MESA, the MESA is defined using standard photolithography and a reactive ion etching step is then used to etch and define the MESA vertically.

The substrate has a photoresist pattern of the MESA etch level. This photoresist is hardened by baking at 115° C for 12 hours. The hardening of the photoresist makes the photoresist more resilient to future etching. The sample is then placed in the reactive ion etcher. The RIE process is described in the seven steps below:

1. Chamber clean

An oxygen RF plasma maintained at load power of 220 watts is activated in the RIE chamber and maintained for 15 minutes. This step is performed before the sample is introduced into the chamber. The oxygen plasma cleans the walls of the chamber and also warms the chamber so that water vapor condensation on the walls is checked.

2. Wafer load

The substrate is then loaded into the chamber.

3. Nitrogen clean

Similarly to the Chamber clean, a nitrogen plasma is ignited at 220 watts and maintained for 2 minutes to further remove contaminants from all surfaces.

4. Sample ashing

A weak (50 W) oxygen plasma is maintained for 1 minute to remove any organic contaminants on the wafer surface.

5. Silicon Tetrachloride flow

$SiCl_4$ gas is allowed to purge the chamber for 20 minutes so that other gases are displaced from the chamber.

6. RIE etching

A $SiCl_4$ plasma is ignited and maintained at 100 watts power for a calculated amount of time. The etch rate for GaN is 287 angstroms per minute. The rate for BN is about 50% higher. $SiCl_4$ does attack photoresist, but at a much slower rate, so that the etch mask essentially remains intact during the etching.

7. Photoresist removal

Finally, an oxygen plasma of 150 watts power is used to completely remove all photoresist from the substrate. The use of reactive ion etching in MESA isolation has worked excellent producing MESA to MESA resistance at greater then 1 MOhm. The use of RIE to etch the individual device layers produces excellent profiles. Figure 14 shows a grating in GaN produced using RIE where the interline spacing is

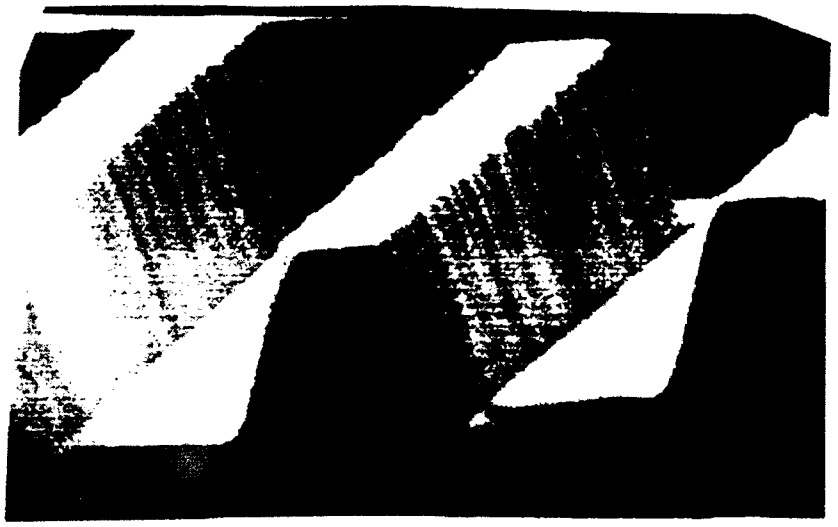

Figure 14. RIE grating profile in GaN.

0.4 microns. These gratings illustrate the successful definition of submicron structures and will be indispensable in future devices where the dimensions will approach submicron levels.

2.6.2 Tungsten Sputter Deposition

The ohmic source and drain contacts will be made by tungsten film liftoff. A photoresist pattern is made on the substrate with a dark field mask, i.e., the ohmic contact areas are open in the pattern. The process sequence for the tungsten deposition is as follows:

1. Sample Load and Pumpdown

The substrate is placed on a water cooled plate under the sputtering target inside the vacuum chamber of the sputtering system. A shutter is placed between the target and the sample. The chamber is then pumped out to a pressure of 10^{-7} Torr to ensure removal of all atmospheric gases.

2. Presputter

A 5 sccm flow of Argon gas is allowed into the chamber and the pressure inside is maintained at 10 milliTorr. An argon plasma is ignited with an input RF power of 50 W going to the target. This plasma initiates sputtering of tungsten atoms from the target surface. This process is maintained for 15 minutes to obtain an oxide-free surface on the tungsten target.

3. Tungsten Deposition using Sputter Proces

The sputtering process is identical to the pre-sputter. The shutter between the target and the substrate is opened to begin the sputtering process. A total of 1000 angstroms of tungsten is obtained in 6 minutes of sputtering.

4. Tungsten Liftoff and Ohmic Contact Definition

The substrate is then immersed in SHIPLEY 1165 photoresist remover at 85° C for 15 minutes. This dissolves out the photoresist and lifts off the tungsten metal in the unwanted areas, leaving behind the desired ohmic contact pattern.

2.6.3 Ohmic Contact Annealing

The as deposited tungsten contacts were not ohmic. Rapid Thermal Annealing (RTA) was performed to anneal these at 1100° C for 20 seconds to convert them to ohmic contacts. The method of TLM, transmission line model, was used to evaluate the specific contact resistivity of these contacts and the contact resistance. Figure 15 illustrates typical TLM measurement results for annealed contacts. The resistance of the contacts are recorded for an increasing separation of contacts and are plotted in a

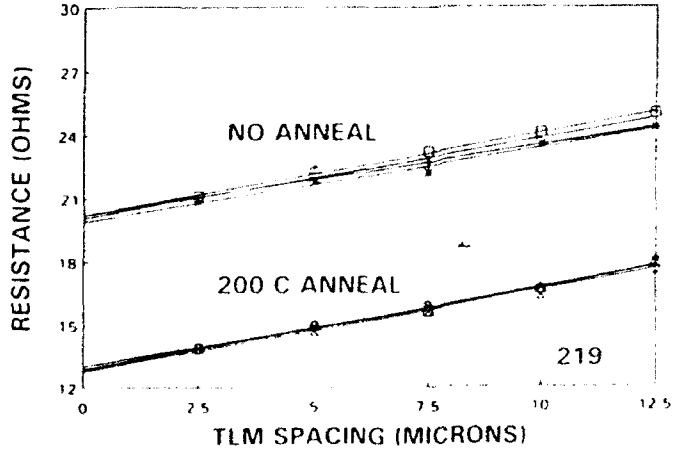

Figure 15. TLM measurements for ohmic contacts to GaN.

resistance vs distance plot. The y intercept along with the area of the contacts allows for the determination of the specific contact resistivity. We are currently measuring a contact resistivity for these contacts around 10^{-4} ohm-cm^{-2}. We are continually improving the ohmic contact metallization procedure and expect the overall specific contact resistivity to decline an order of magnitude.

2.6.4 Ion Implantation for MESA Isolation

Although RIE defines the MESA's and physically separates them from other MESA's, the MESA's are still connected by RIE surface. Following the definition of MESA's using RIE, it was discovered that the MESA's were still not electrically isolated. The cause of the poor isolation is thought to be a conductive skin left near the surface following reactive ion etching. To isolate the MESA's we have developed an ion implantation scheme.

Figure 16 illustrates the process of multiple ion implantation. By using implants of various dosages and at various energies, the depth and concentration of the implants can be controlled. By using a combination of implants a desired profile can be obtained as a function of depth. The use of this implantation technique has worked excellent yielding MESA's with Mohm resistances between MESA's.

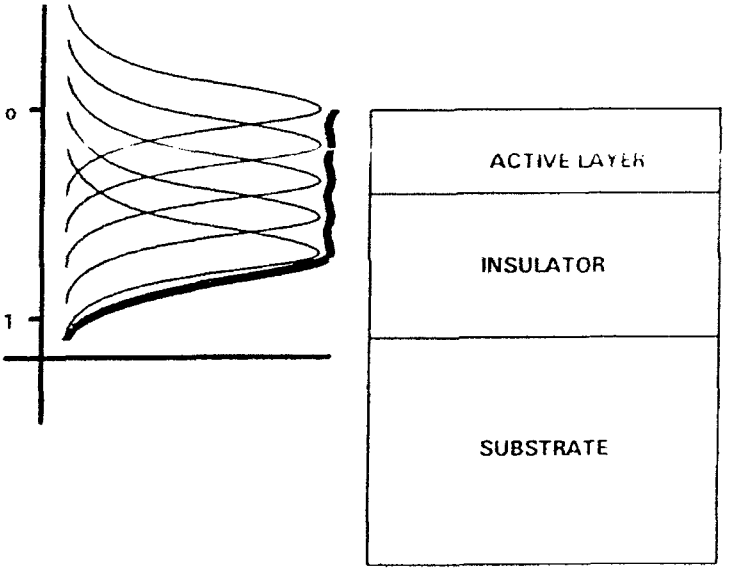

Figure 16. Multiple Ion implant carrier profile in GaN.

3.0 Summary

In summary we successfully accomplished atomic layer epitaxy of hexagonal boron nitride films over sapphire and silicon substrates. Insights were gained into the BN deposition process and growth kinetics.

We also established the feasibility of using BN layers over $Al_xGa_{1-x}N$ - GaN MISFET structures. Based on these we plan to develop BN - $Al_xGa_{1-x}N$ based transistor devices in the Phase II program.